View metadata, citation and similar papers at core.ac.uk
brought to you by CORE
provided by Jakov - Repository of the University of Criminal Investigation and Police Studies, Belgrade

Science of Sintering, **50** (2018) 225-235

doi:https://doi.org/10.2298/SOS1802225K

UDK 675.92.027

Inversion Charge Density of MOS transistor with Generalized Logistic Functions

Tijana Kevkić[1*)], Vladica Stojanović[1], Vera Petrović[2], Dragan Ranđelović[3]

[1]Faculty of Science and Mathematics, University of Priština (in Kosovska Mitrovica), Lole Ribara 29, 38220 Kosovska Mitrovica, Serbia
[2]School of Electrical Engineering and Computer Science of Applied Studies, Vojvode Stepe 283, 11000 Belgrade, Serbia
[3]Academy of Criminalistics and Police Studies, Cara Dušana 196, Belgrade, Serbia, 11000 Belgrade, Serbia

Abstract:

In this paper, the expression for the charge density in inversion layer at the surface of semiconductor has been improved. The improvement is related to the replacement of an empirical smoothing factor by new one which has generalized logistic (GL) functional form. The introduction of the GL function of the second type in the original interpolating expression leads to continual and smooth transition of the inversion charge density (ICD) between different regions of metal-oxide-semiconductor (MOS) operation. Moreover, in this way any empirical determinations are avoided. The simulated values of the ICD match closely with the numerical results of implicit charge sheet model for a wide range of dopant concentration and oxide thickness. In addition, the proposed GL fitting procedure has been also extended in the case where quantum mechanical effects play important role in inversion mode of scaled MOS devices.

Keywords: *Inversion charge density; MOS modeling; Generalized logistic function; Quantum mechanical effects.*

1. Introduction

The MOS structure is most useful device in the study of electrical properties of semiconductor's surface. Almost universally, it utilizes doped silicon as the substrate and its native oxide, silicon dioxide. There is no carrier transport through the oxide because the insulating quality of the SiO_2 is quite good [1]. When a small positive voltage is applied between the metal and the semiconductor of p-type, bands bend downward near the Si-SiO_2 interface, and majority carriers are depleted [2, 3]. By increasing the applied voltage, the band bending becomes large enough that concentration of minority carriers (electrons) exceeds the concentration of majority carriers (holes) and the semiconductor surface enters the inversion regime. At still larger applied voltage, we finally arrive at a situation in which the electron volume concentration at the surface of Si exceeds the doping density in it [4, 5]. This is the strong inversion case in which a significant conducting sheet of inversion charge is formed at

*) **Corresponding author:** tijana.kevkic@pr.ac.rs

the Si-SiO_2 interface.

Since the basis for operation of the MOS devices is the ability to induce and modulate a conducting sheet of minority carriers at the interface, the obtaining of one single expression for the inversion charge density (ICD), valid for all regions of operation is very important. On the other side, the ICD in the depletion and weak inversion has functional dependence on the external voltage different from that in strong inversion. That is why the usage of the same functional form for both of these charge densities over the entire operating range is not desirable. Therefore, these two components should be separated [6] and an interpolating curve to bridge the gap between weak and strong inversion should be introduced [7, 8]. Unfortunately, commonly used interpolating functions are nonphysical [9] or contain empirical parameters [10] for achieving the continuity and smoothness of the ICD at the boundary points.

In order to obtain the explicit expression for the ICD with no empirical parameters, valid in whole useful region of the MOS operation, here we introduce the so-called Generalized Logistic (GL) functions of the second type in fitting of the mentioned smoothing factor. Thanks to the GL functions the obtained ICD is perfectly continuous with respect to external voltage V_G over the entire MOS operating range. Improvement of original explicit expression [11] with this new GL form for smoothing factor has been confirmed by extensively comparisons with results of the implicit charge sheet based model for wide range of Si substrate doping and SiO_2 thickness. Moreover, the continuous trend towards smaller, faster and cheaper devices leads to increased complexity of devices and significant reduction of their dimensions [12]. In scaled devices quantum mechanical effects (QME) reduce ICD for the same applied voltages as compared to the classical theory, and also change other device parameters. The similar GL procedure can be incorporated in the compact MOS model which takes into account the QME in an approximate and efficient manner.

2. General analysis for inversion charge density

Consider the MOS transistor with p-type semiconductor homogenously doped with an acceptor concentration of N_A, and SiO_2 insulating layer which thickness is t_{ox}. Under the assumption of the gradual channel and charge sheet approximations, in the useful range of MOS operation (depletion and inversion), the electrostatic surface potential is related to the gate voltage V_G through the following implicit relation [13]:

$$V_G = V_{FB} + \psi_s + \gamma \sqrt{\psi_s + u_T \cdot \exp\left(\frac{\psi_s - 2\phi_F - V_{ch}}{u_T}\right)}. \quad (1)$$

Here:

- V_{FB} is flat-band voltage,
- $\gamma = \sqrt{2q\varepsilon_{Si}N_A} / C_{ox}$ is the substrate body factor, where $C_{ox} = \varepsilon_{ox} / t_{ox}$ is the oxide capacitance per unit area,
- $u_T = kT / q$ is the thermal potential,
- $\phi_F = u_T \ln(N_A / n_i)$ is Fermi potential in the substrate,
- V_{ch} is channel potential defined by the difference between the quasi-Fermi potentials of the carriers forming the channel (ϕ_n) and that of the majority carriers (ϕ_p).

Solving Eq. (1) requires numerical techniques and ψ_s cannot be explicitly found as a function of V_G . Applying Gauss theorem at the interface gives the relation between the ICD Q_I and the surface potential ψ_s in following form:

$$Q_I = -\gamma \cdot C_{ox} \cdot \left(\sqrt{\psi_s + u_T \cdot \exp\left(\frac{\psi_s - 2\phi_F - V_{ch}}{u_T} \right)} - \sqrt{\psi_s} \right). \tag{2}$$

From Eq. (2) is clear that Q_I remains an implicit function of the gate voltage V_G through the ψ_s. Nevertheless, the values of Q_I obtained from Eq. (2) with numerical solutions of Eq. (1) for ψ_s serve as corresponding benchmark results for the inversion charge density. From the circuit modeling of view the explicit formulations of ψ_s and Q_I are preferable because of their simplicity and fast computational speed. An attempt for analytical determination of the ψ_s has been made in [13] by considering the weak and strong inversion as two different regions of MOS operation.

In the strong inversion region $(\psi_s > 2\phi_F + 2V_{ch})$, the exponential term in Eq. (1) is dominant and surface potential becomes almost constant:

$$\psi_{s_{si}} = \psi_0 + V_{ch}, \tag{3}$$

where ψ_o is a potential at the onset of strong inversion. Replacing ψ_s with $\psi_{s_{si}}$ in Eq. (2) leads to a linear approximate expression for the ICD in strong inversion region:

$$Q'_{I_{si}} = -C_{ox} \cdot (V_G - V_T). \tag{4}$$

Here, V_T is the gate threshold voltage referred to the local substrate, defined as:

$$V_T = V_{FB} + \psi_0 + V_{ch} + \gamma \cdot \sqrt{\psi_0 + V_{ch}}. \tag{5}$$

In the weak inversion region $(\psi_s < 2\phi_F + V_{ch})$, the exponential term in Eq. (1) is negligible and the surface potential can be approximated by:

$$\psi_{s_{wi}} = \left(-\frac{\gamma}{2} + \sqrt{V_G - V_{FB} + \frac{\gamma^2}{4}} \right). \tag{6}$$

The inversion charge density in the weak inversion can be given by the following approximate relation:

$$Q'_{I_{wi}} = -(n-1) \cdot C_{ox} \cdot u_T \cdot \exp\left(\frac{V_G - V_T}{n \cdot u_T} \right). \tag{7}$$

Here, n is the inverse slope of $\psi_{s_{wi}}$ versus V_G characteristics in the weak inversion region.

3. Inversion charge density modeling

The ICD linearly depends on the voltage V_G in strong inversion region, while that dependence is exponential in the subthreshold region. One simple explicit expression for the ICD, which is beneficial for the convergence properties of the circuit simulation programs, can be obtained by introducing the interpolating function. The simple interpolating function has been proposed originally in [11] giving the resulting expression for the ICD in the following form:

$$Q'_{inv} = -K \cdot C_{ox} \cdot u_T \cdot \ln\left[1 + \exp\left(\frac{V_G - V_T}{n \cdot u_T}\right)\right]. \tag{8}$$

Here, K is the smoothing factor which insures a continuous transition of the ICD between weak and strong inversion region. Namely, in weak inversion Eq. (8) reduces to

$$Q'_{inv} \approx -K \cdot C_{ox} \cdot u_T \cdot \exp\left(\frac{V_G - V_T}{n \cdot u_T}\right), \tag{9}$$

while into strong inversion it takes next form

$$Q'_{inv} \approx -\frac{K}{n} \cdot C_{ox} \cdot (V_G - V_T). \tag{10}$$

Comparing Eq. (9) with Eq. (7), and Eq. (10) with Eq. (4), we see that Eq. (8) can be used to predict the values of the ICD in whole useful region of MOS operation if the factor K varies smoothly from n 1 in depletion and weak inversion region to n as a threshold voltage is approached. In [10] is proposed the following form for K versus gate voltage:

$$K_m(V_G) = n + \frac{1}{2}\left(-1 + \frac{V_G - V_T}{\sqrt{(V_G - V_T)^2 + \varepsilon^2}}\right), \tag{11}$$

where ε is an empirical parameter which takes values between 0.2V and 0.8V. However, several simulations have shown that the ICD values obtained from Eq. (8) with the smoothing factor K_m deviate significantly from those obtained from the implicit charge sheet (CS) solution, particularly in the weak inversion region [14]. The cause of the deviation comes from a purely empirical nature of the factor K_m, i.e. from neglecting of the fact that manner and speed of K (and consequently of ICD) transition are sensitive to changes in technological and physical characteristics of the MOS devices [15].

In order to eliminate these deviations, and take into account the mentioned sensitivity of transition, here we propose the following functional form for factor K:

$$K_{GL}(V_G) = (n-1) + I_{GL}(V_G), \tag{12}$$

where

$$I_{GL}(V_G)=1-\left[1+b\cdot\exp\left(\frac{a}{u_T}(V_G-V_T)\right)\right]^{-\frac{1}{\nu}} \tag{13}$$

is *the Generalized Logistic function (of the second type)*. The parameters *a, ν > 0* are usually named *the growth parameters* because the growth of GL-curve directly depends on them. The third parameter *b>0* determines the shift of GL-curve, which is related to the value $I_{GL}(V_T)=1-(1+b)^{-1/\nu}$.

Substitution of $I_{GL}(V_G)$ in Eq. (12) gives *the GL-fitted* factor $K_{GL}(V_G)$ in the next form:

$$K_{GL}(V_G)=n-\left[1+b\cdot\exp\left(\frac{a}{u_T}(V_G-V_T)\right)\right]^{-\frac{1}{\nu}}. \tag{14}$$

According to Eqs. (12)-(14), inequality $I_{GL}(V_G)\approx 0$ implies $K_{GL}(V_G)\approx n-1$ (for $V_G<V_T$), while for $I_{GL}(V_G)\approx 1$ follows $K_{GL}(V_G)\approx n$ (for $V_G>V_T$).

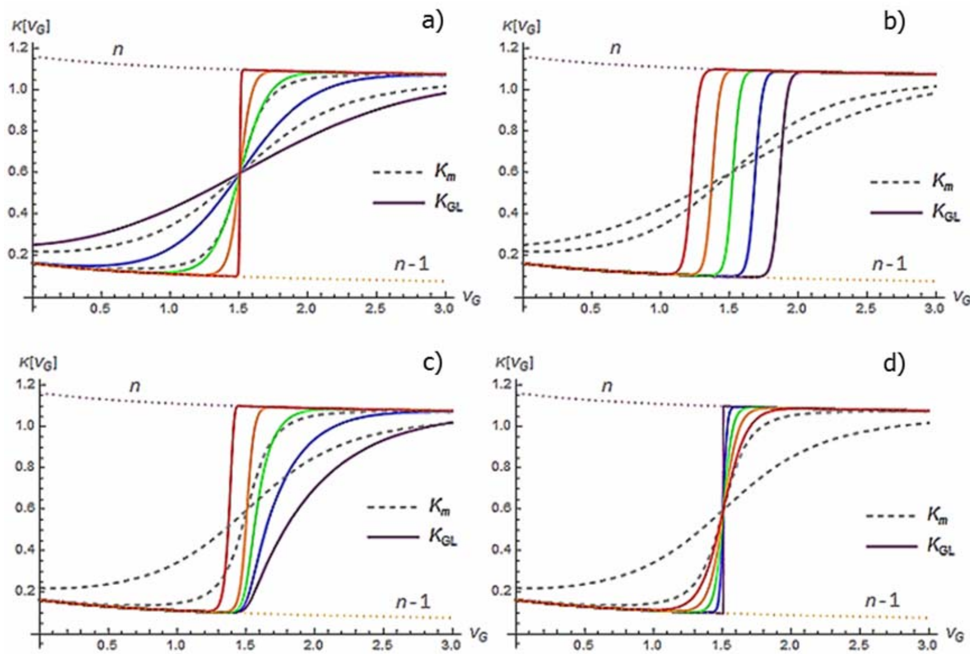

Fig. 1. Graphs of the GL-fitting of the parameter *K*, by using the Eq. (14) (solid lines), compared to the fitting model proposed in Eq. (11) (dashed lines): a) Varying of the parameter *a* ($\nu = b = 1$, $u_T = 0.026$). b) Varying of the parameter *b* ($a = \nu = 1$, $u_T = 0.026$). c) Varying of the parameter *ν* ($a = b = 1$, $u_T = 0.026$). d) Varying of the parameter u_T ($a = \nu = b = 1$).

The variation of the values of $K_{GL}(V_G)$ for varying values of the parameters *a,b,ν*, as well as the thermal voltage u_T is shown in Fig. 1. The graphs of $K_m(V_G)$ for $\varepsilon = 0.2$V and $\varepsilon = 0.8$V, are also shown in this figure for comparison. As we can see, the GL model's parameters

a,b,v completely control the rate of change and the smoothness of the function $K_{GL}(V_G)$. Let us notice that, for instance, if $a >> u_T$ and $\nu \approx 0$ there is a rapid transition of $K_{GL}(V_G)$ values from n 1 to n. On the other hand, the transition of $K_{GL}(V_G)$ becomes smoother and slower by reducing the value of the ratio *a*/*v* as is shown in Fig. 1 (left diagrams). Unlike the function $K_m(V_G)$ proposed in [10], the introduction of GL function offers $K_{GL}(V_G)$ transitions with great versatility and adaptability. Moreover, the constraints related to empirical determination of the smoothing parameter ε in Eq. (11) are avoided.

4. Results for inversion charge density

The GL-model's parameters *a*, *b*, ν, as well as of the intercept ln*b*, have been estimated for MOS transistor whose technological and physical characteristics are shown in Tab. I. Additionally, coefficient of determination (R^2) and the Akaike's Information Criterion (AIC) as typical goodness-of-fit scores have been also estimated. They present the quality fitting of the theoretical model with the real-based data.

Tab. I MOS's characteristics and estimated values of the GL-fitted model's parameters.

Items	Values
t_{ox}	2.5nm
N_A	5×10^{17} cm^{-3}
$2\ _F$	0.88826V
V_{ch}	0.0000V
V_T	0.3857V
γ	0.2890V$^{-1/2}$
C_{ox}	0.0138Fm^{-2}
a	0.9165
ln b	-0.4130
b	0.6617
v	10
R^2	0.9546
AIC	-104.2

As can be seen the estimated value of R^2 is higher than 95 %, while AIC estimate takes negative value. This indicates the high-level performance of the GL-fitted factor K_{GL}, and justifies its introduction in the interpolating relation (8).

The ICD obtained from Eq. (8) with K_m and K_{GL}, respectively, are shown in Fig. 2 along with the numerical solutions of Eq. (2) and results of the strong inversion approximation given by Eq. (4). From this figure is clear that Eq. (8) with K_{GL} gives an accurate description of inversion charge density in whole inversion region. This also confirms Tab. II which shows the absolute errors (*AE*) and fractional errors (*FE*) in modeled inversion charge density and fitted factor *K*, taking the CS results as reference. All errors have been computed for MOS device from Tab. I, separately for weak and strong inversion region, as well as in the whole region of approximation.

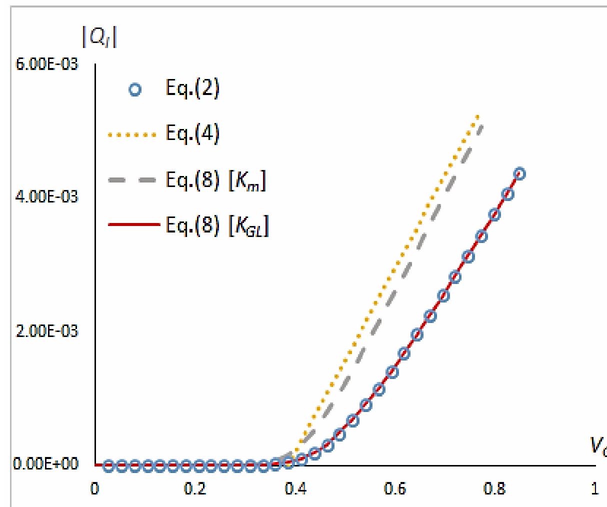

Fig. 2. Various types of ICD approximations vs. V_G. The results of Eq. (2) are taken as reference values (dots).

As we can see from the Tab. II, all the estimated errors are significantly lower in the case of GL-fitted parameter. For instance, maximum fractional error occurs in the strong inversion region with a value of only 0.71 %. It is exactly 83 times less than corresponding FE value with K_m. This is also apparent from Fig. 3 where are shown, in the logarithmic scales, the absolute errors $AE = |Q'_I - Q'_{inv}|$, as well as the fractional errors $FE = \frac{|Q'_I - Q'_{inv}|}{|Q'_I|}$ of the both mentioned ICD-approximations.

Tab. II Estimated errors obtained by various types of the *K*-fitting and the ICD-fitting values.

Errors	Regions	*K*-fitting		ICD-fitting (Q'_{inv})	
		Eq.(11) [K_m]	Eq.(14) [K_{GL}]	Eq.(8) [K_m]	Eq.(8) [K_{GL}]
AE	Weak inversion	1.49E-01	8.01E-04	5.49E-06	1.14E-08
	Strong inversion	3.30E-01	4.66E-03	1.61E-03	3.33E-05
	Whole region	2.79E-01	3.58E-03	1.13E-03	2.34E-05
FE	Weak inversion	85.93%	0.46%	85.93%	0.46%
	Strong inversion	58.93%	0.71%	58.93%	0.71%
	Whole region	70.20%	0.70%	65.94%	0.62%

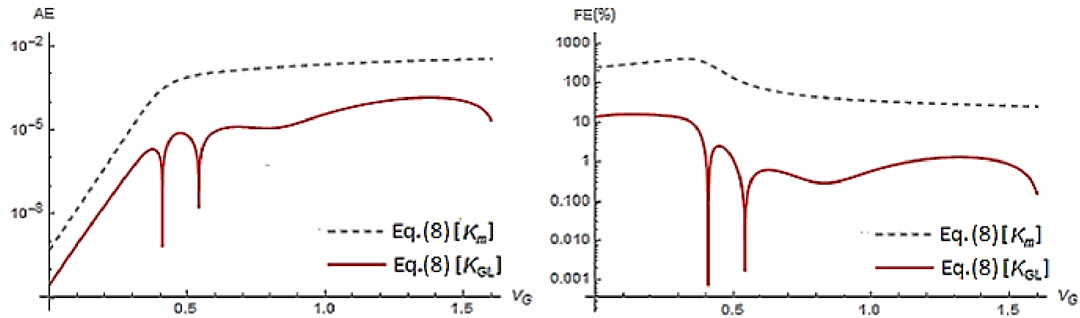

Fig. 3. Absolute errors (left diagram) and fractional errors (right diagram) of the ICD-approximations $|Q'_{inv}|$ vs. gate voltage V_G with two K-fitted parameter: K_m (dashed line) and K_{GL} (solid line).

5. Modeling of the ICD decrease due to the energy quantization

The GL functions can be also implemented in the MOS models which include the energy quantization of carriers in inversion layer of scaled devices. The quantization is primarily caused by high substrate doping and small effective oxide thickness. Namely, these two factors often cause forming of a narrow potential well at the Si-SiO_2 interface. The Si conduction band splits into discrete energy levels with the most of electrons responsible for current transport in inversion layer residing in the lowest level. The concentration of these electrons can be found by solving Schrödinger equation, while their charge distribution must also satisfies Poisson equation [16, 17]. Thus, Schrödinger and Poisson (SP) equations are coupled here and need to be solved self-consistently. Variational approach applied to solving SP system gives quantum mechanically QM corrected surface potential $\psi_{s[qm]}$ [18].

Replacing classical surface potential ψ_s by $\psi_{s[qm]}$ in Eq. (2) results in quantum mechanical (QM) modified ICD:

$$Q'_{I[qm]} = -\gamma \cdot C_{ox} \cdot \left(\sqrt{\psi_{s[qm]} + u_T \cdot \exp\left(\frac{\psi_{s[qm]} - 2\phi_F - V_{ch}}{u_T} \right)} - \sqrt{\psi_{s[qm]}} \right). \tag{15}$$

On the other hand, the interpolating ICD model which takes into account energy quantization [10] gives ICD in following form:

$$Q'_{inv[qm]} = -K_{m[qm]} \cdot C_{ox} \cdot u_T \cdot \ln\left[1 + \exp\left(\frac{V_G - V_{T[qm]}}{n \cdot u_T} \right) \right], \tag{16}$$

where $K_{m[qm]}$ is QM modified smoothing parameter obtained from Eq. (11) with QM-modified threshold voltage $V_{T[qm]}$, given by

$$V_{T[qm]} = V_{FB} + 2\phi_F + V_{ch} + \delta\psi_s + \gamma\sqrt{2\phi_F + V_{ch} + \delta\psi_s}\ . \tag{17}$$

Here, we propose introduction of QM modified GL-fitted parameter $K_{GL[qm]}$ obtained from Eq. (15), with the threshold voltage $V_{T[qm]}$ given by Eq. (17):

$$Q'_{inv[qm]} = -K_{GL[qm]} \cdot C_{ox} \cdot u_T \cdot \ln\left[1 + \exp\left(\frac{V_G - V_{T[qm]}}{n \cdot u_T}\right)\right]. \quad (18)$$

In order to clearly portray the ICD behavior over the entire range of MOS operation, the results of Eq. (16) and Eq. (18) are shown in Fig. 4. The results of Eq. (15) are taken as reference values. The result of classical Eq. (2) is also shown for comparison, and as can be seen the classical value of the ICD is obvious higher than the QM-modified one.

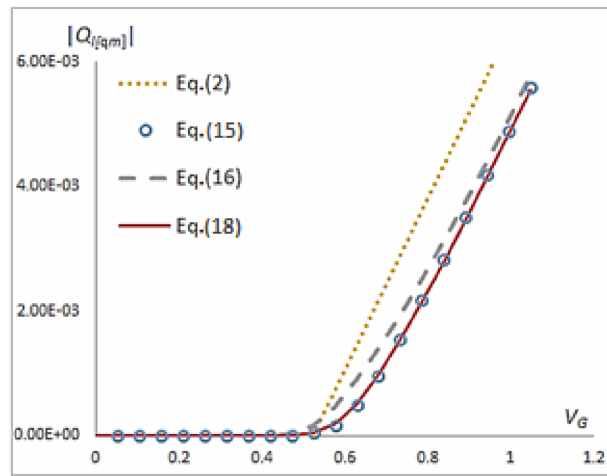

Fig. 4. The inversion charge density vs. terminal voltage V_G as obtained from the: Classical model (dotted line), QM incorporated explicit ψ_s - model (dots) and two Interpolating QM-modified ICD models (dashed and solid lines).

A good match between the results of Eq. (18) and reference values proves that QM-modified ICD interpolating relation with GL fitted smoothing factor takes into account influence of QME on the ICD in whole inversion region more precisely than the model proposed in [10]. Furthermore, the absolute (AE) and fractional (FE) errors in QM modified ICD obtained from Eq. (16) and Eq. (18), taking the results of Eq. (15) as reference, are shown in the Tab. III. As in the classical case, all errors are significantly lesser in the case of GL fitted smoothing factor *K*. Moreover, notice that in the case of Eq. (18) the increasing of the gate-voltage V_G implies that AE and FE tend to zero. This can be clearly observed from Fig. 5, where the diagrams of AE and FE are shown, in the logarithmic scales, for both of the above QM interpolating ICD relations (16) and (18).

Tab. III Estimated errors of interpolating ICD-models with different choices of parameter *K*, compared to the reference QM-incorporated ICD- model.

Estimated errors	Interpolated QM-modified ICD-model $(Q'_{inv[qm]})$	Reference QM-incorporated ICD- model $(Q'_{I[qm]})$		
		Weak inversion	Strong inversion	Whole region
AE	Eq. (16)	2.98E-06	5.25E-04	4.23E-04
	Eq. (18)	1.02E-07	5.34E-05	4.28E-05
FE	Eq. (16)	184.32%	11.64%	50.24%
	Eq. (18)	14.43%	1.06%	3.72%

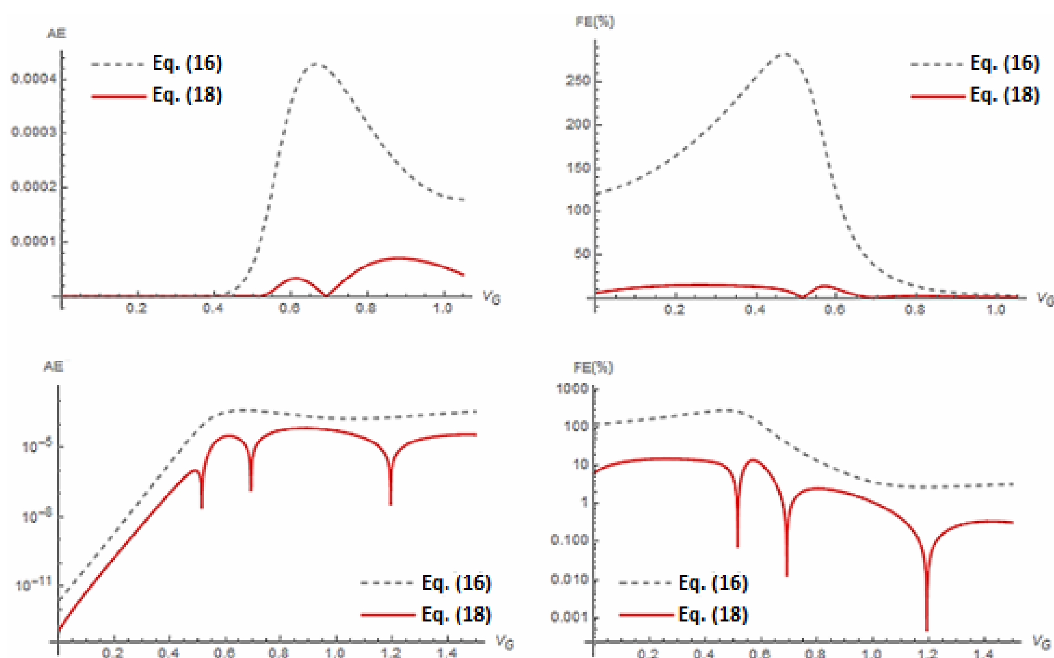

Fig. 5. Graphics of the absolute errors (left diagrams) and the fractional errors (right diagrams) for Interpolating QM-modified ICD-models given in Eq. (16) (dashed lines) and Eq. (18) (solid lines).

6. Conclusion

New form for the smoothing factor which controls the continuity of the inversion charge density in entire useful range of MOS operation has been proposed. It is based on generalized logistic function of second type and provides completely control of continuity, smoothness as well as speed and manner of the ICD transition between weak and strong inversion region. Results of the original explicit expression for ICD with the GL fitted factor show good match with the numerical results of the classical implicit charge sheet based model. Moreover, the developed GL-approach can be also broaden in the case of scaled MOS devices where the quantum mechanical effects become significant.

7. References

1. Chaudhry, J. N. Roy, Electron, 14 (2) (2010) 86.
2. P. Vimala, N. B. Balamurugan, J. Semicon, 34 (11) (2013) 114001.
3. W. Wu, W. Yao, G. Gildenblat, Solid-State Electron., 54(5) (2010) 595.
4. K. Jia, W. Sun, Microelectron. J., 42 (10) (2011) 1169.
5. N. Shigyo, IEEE Trans. Electron Dev., 49 (7) (2002) 1267.
6. Z. Arefinia, Mater. Sci. Semicon. Proceed., 16 (2013) 1240.
7. G. Montoro, M. Schneider, V.C. Pahim, R. Rios, NSTI-Nanotech, (2005) 13-18.
8. Y. P. Tsividis, Operation and modeling of the MOS transistor, 2nd Ed., Oxford University Press, 1999.

9. H. Pal, K. D. Cantley, S. S. Ahmed, M. S. Lundstrom, IEEE Trans. Electron. Dev., 55 (2008) 904.
10. Basu, A. Dutta, Solid-State Electron., 50 (2006) 1299.
11. H. J. Oguey, S. Cserveny, in: "Summer Course on Process and Device Modeling. ESAT Leuven-Heverlee", Belgium, (1996) 555-558.
12. Z. Stanimirović, I. Stanimirović, Sci. Sinter., 49 (2017) 91.
13. R. van Langevelde, F. M. Klaassen, Solid-State Electron., 44 (2000) 409.
14. T. Kevkić, V. Stojanović, Lj. Spalević, in: "24th International Electrotechnical and Computer Science Conference ERK", 2015, p. 15-18.
15. T. Kevkić, V. Stojanović, D. Joksimović, J. Comput. Electron. 16 (2017) 90.
16. M. J. van Dort, P. H. Woerlee, A. J. Walker, Solid-State Electron. 37(3) (1994) 411.
17. B. P. K. Yadav, A. Dutta, J. Semicon. Tech. Sci., 10:3 (2010) 203.
18. L. F. Mao, Pramana J. Phys., 72 (2) (2009) 407.

Садржај: *Израз за густину наелектрисања у инверзном слоју на површини полупроводника побољшан је у овом раду. Побољшање је постигнуто заменом емпиријског фактора глаткости новим параметром који има облик уопштене логистичке функције. Увођење уопштених логистичких функција другог реда у оригинални интерполациони израз обезбеђује континуални и глатки прелаз густине инверзног наелектрисања између различитих области рада MOS транзистора. Поред тога, на овај начин су избегнута било каква емпиријска одређивања. Израчунате вредности густине наелектрисања показују одлично слагање са нумеричким резултатима имплицитног модела наелектрисања слојева за широк опсег концентрације примеса и дебљине оксида. Додатно, предложени поступак фитовања проширен је и на случај MOS уређаја смањених димензија на чији рад значајни утицај имају квантно механички ефекти.*
Кључне речи: *Густина наелектрисања инверзног слоја; MOS моделирање; уопштена логистичка функција; квантно механички ефекти.*

© 2016 Authors. Published by the International Institute for the Science of Sintering. This article is an open access article distributed under the terms and conditions of the Creative Commons — Attribution 4.0 International license (https://creativecommons.org/licenses/by/4.0/).